

Supporting information

Isolation and characterization of antimicrobial peptides with unusual disulfide connectivity from the colonial ascidian *Synoicum turgens*

Ida K. Ø. Hansen ¹, Johan Isaksson ², Aaron G. Poth³, Kine Ø. Hansen ⁴, Aaron J. C. Andersen ¹, Céline S. Richard ¹, Hans-Matti Blencke¹, Klara Stensvåg¹, David J. Craik³ and Tor Haug ¹

- ¹ Norwegian College of Fishery Science, Faculty of Biosciences, Fisheries and Economics, UiT The Arctic University of Norway, Breivika, N-9037 Tromsø, Norway
- ² Department of Chemistry, UiT The Arctic University of Norway, Breivika, N-9037 Tromsø, Norway
- ³ Institute for Molecular Bioscience, The University of Queensland, Brisbane 4072, Queensland, Australia
- ⁴ Marbio, UiT The Arctic University of Norway, Breivika, N-9037, Tromsø, Norway

Table of contents

- Figure S1.** MS spectra of the isotope patterns of the purified peptides
- Figure S2.** MS/MS spectra of the intact peptides of turgencin A and turgencin A_{Mox1}
- Figure S3.** MS/MS spectrum highlighting the different oxidation states of turgencin B
- Figure S4.** Retention times of turgencin A, B and their oxidized derivatives
- Figure S5.** ¹⁵N-HSQC (at natural abundance) of turgencin A_{Mox1} in water
- Figure S6.** ¹⁵N-HSQC (at natural abundance) of turgencin B_{Mox2} in water
- Figure S7.** TALOS+ predicted secondary structure of turgencin B_{Mox2}
- Figure S8.** The ³J_{HNHA} coupling constants of turgencin B_{Mox2}
- Figure S9.** Early test calculations of turgencin B_{Mox2} using crude constraints to evaluate different disulfide patterns using crude constraints
- Figure S10.** The most viable alternative disulfide pattern of turgencin B_{Mox2} compared to the found pattern in terms of energy
- Figure S11.** RMSD relative to the starting frame, energies of the turgencin B_{Mox2} and the RMSF of the backbone during the free MD trajectory
- Figure S12.** Comparison of NMR and molecular dynamics structures for turgencin B_{Mox2}
- Table S1.** Antimicrobial activity of solid phase extract fractions and the organic extract
- Table S2.** Calculated and measured monoisotopic *m/z* [M+4H]⁴⁺ ions of the turgencins
- Table S3.** Proton chemical shift assignments for turgencin A_{Mox1} in water
- Table S4.** Carbon chemical shift assignments for turgencin A_{Mox1} in water
- Table S5.** Proton chemical shift assignments for turgencin B_{Mox2} in water
- Table S6.** Carbon chemical shift assignments for turgencin B_{Mox2} in water
- Table S7.** Peptides sharing the same disulfide connectivity as turgencin B

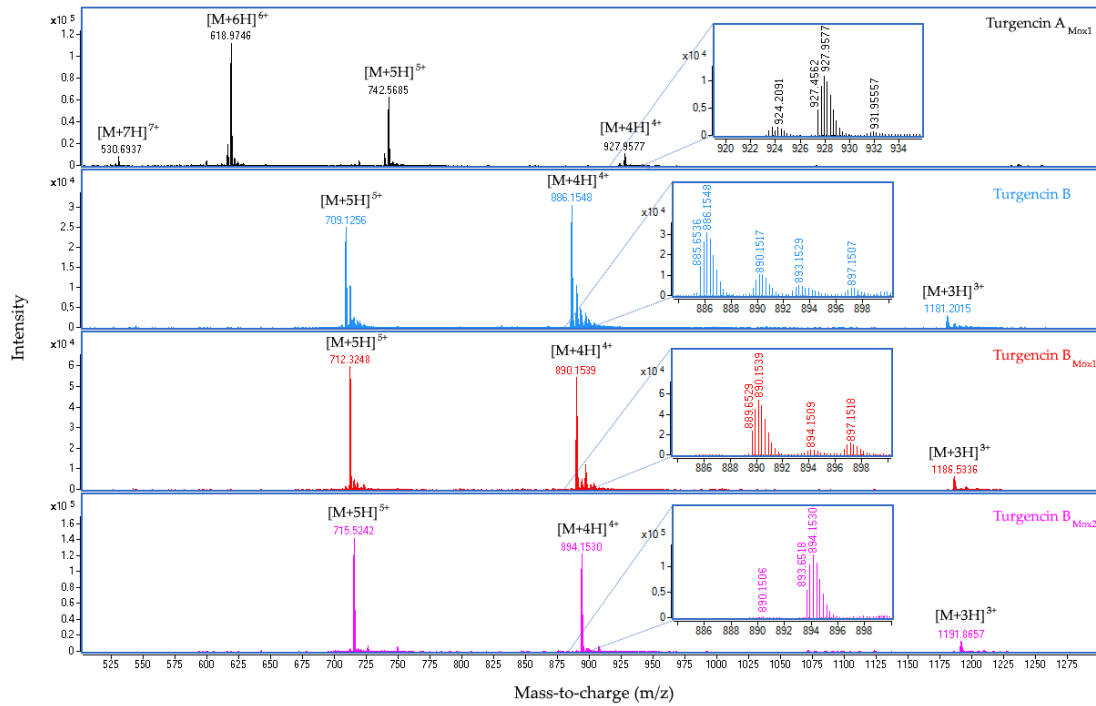


Figure S1. MS spectra of the isotope patterns of the purified peptides turgencin A_{Mox1}, turgencin B, turgencin B_{Mox1} and turgencin B_{Mox2}. The $[M+4H]^{4+}$ ions are highlighted, and the monoisotopic signals of these ions were used for calculation of the monoisotopic masses of the peptides.

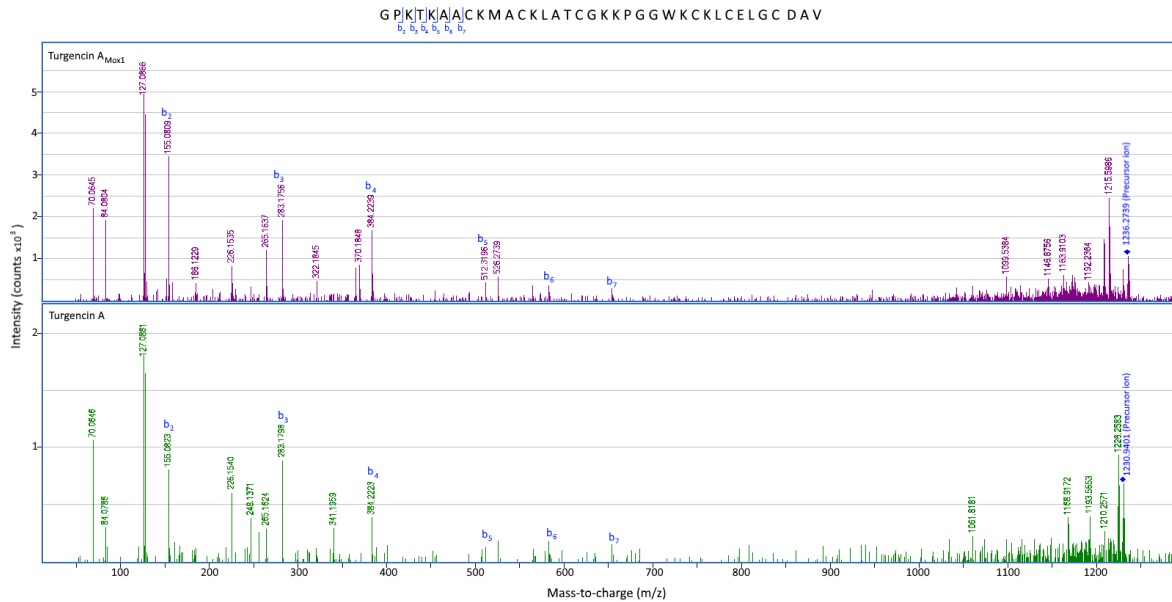


Figure S2. MS/MS spectra of the $[M+3H]^{3+}$ precursor ions m/z 1236.27 and m/z 1230.94 of the intact peptides of turgencin A and turgencin A_{Mox1} respectively.

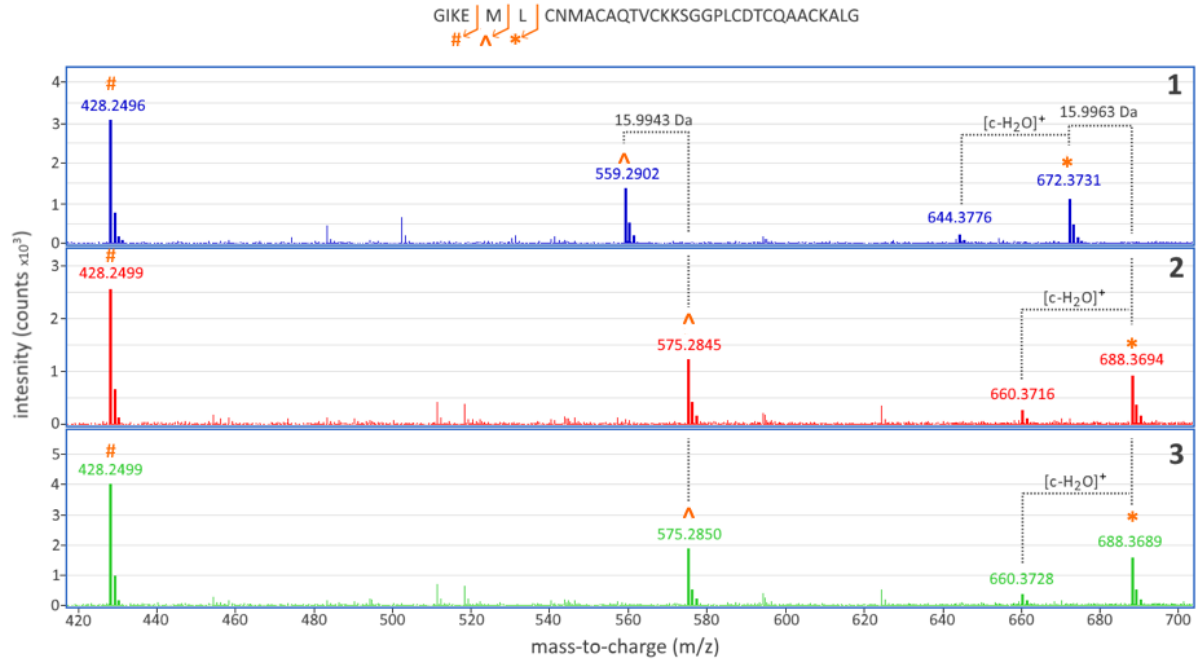


Figure S3. MS/MS spectra of the $[M+4H]^{4+}$ precursor ions, highlighting the differing oxidation states of Met5 across three turgencin B oxiforms, zoomed in between m/z 420-700. Spectrum 1 is of turgencin B (precursor m/z 885.65), spectrum 2 illustrates the oxidation of turgencin B_{Mox1} (precursor m/z 889.65), and spectrum 3 is of turgencin B_{Mox2} (precursor m/z 893.65).

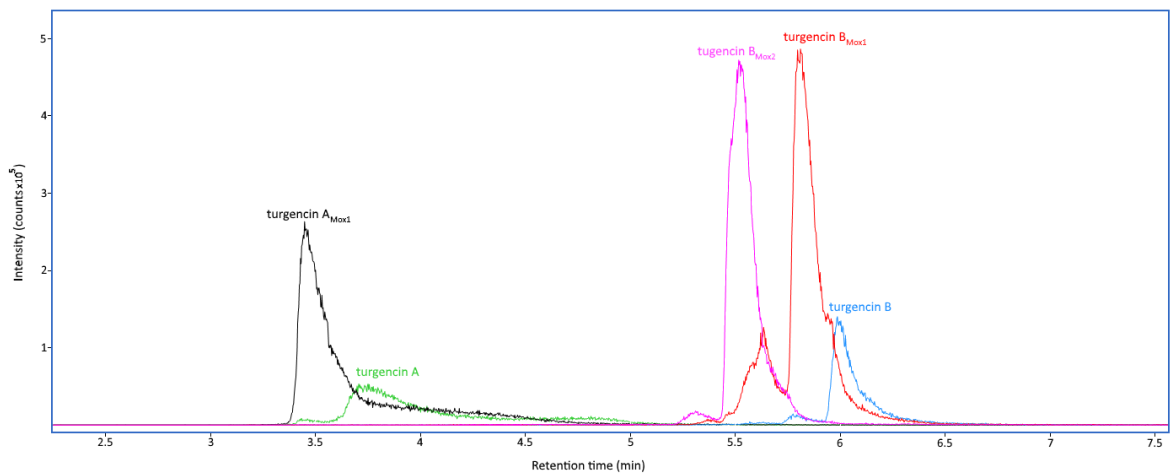


Figure S4. Reversed-phase HPLC separation of turgencin A, B and their oxidized derivatives. Peptides with methionine oxidation exhibit shorter retention times, corresponding with decreased hydrophobicity.

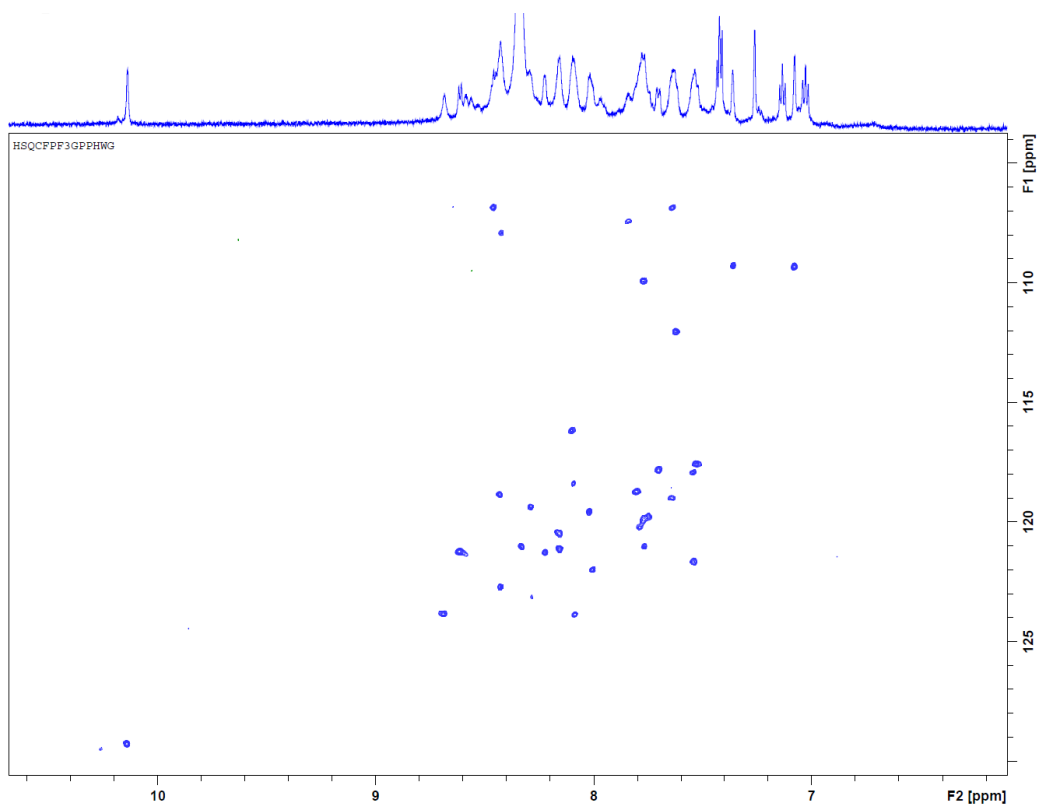


Figure S5. ^{15}N -HSQC (at natural abundance) of turgencin A_{Mox1} in water.

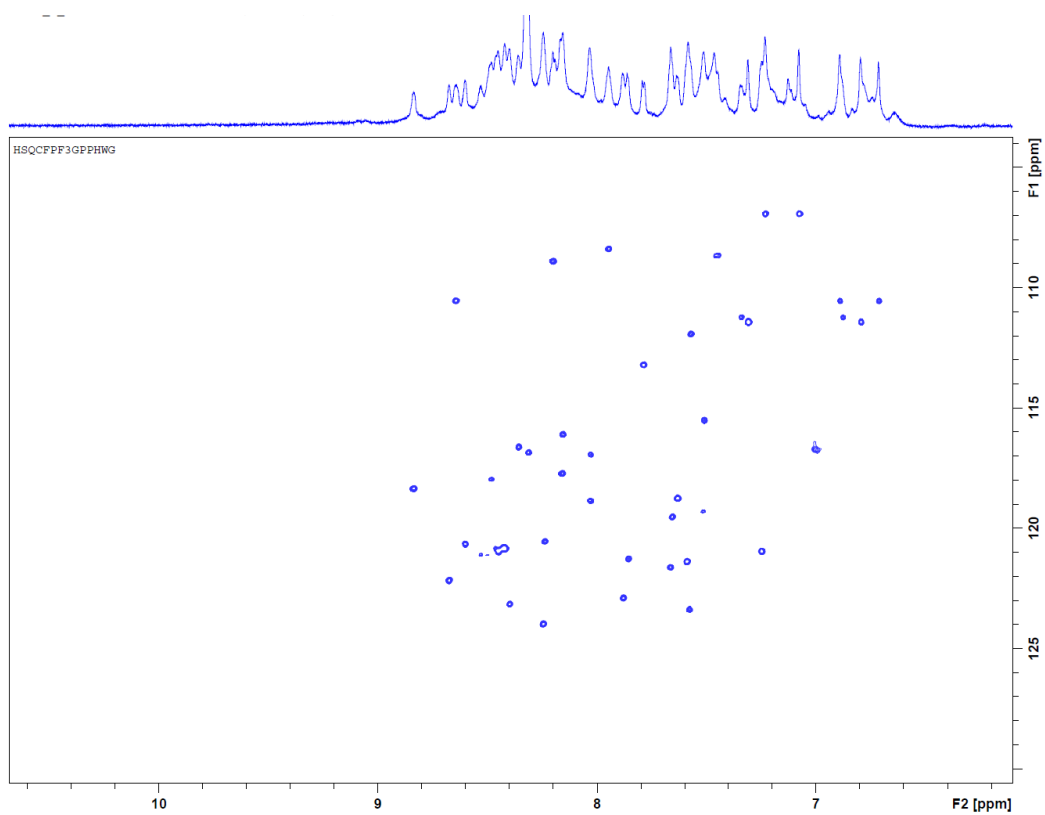


Figure S6. ^{15}N -HSQC (at natural abundance) of turgencin B_{Mox2} in water.

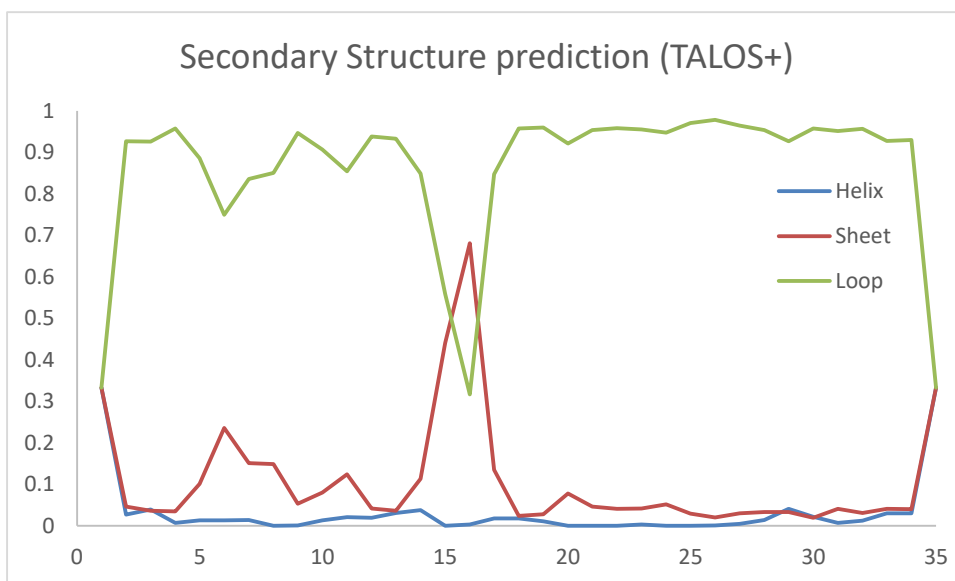


Figure S7. TALOS+ predicted secondary structure of turgencin B_{Mox2} based on all available chemical shifts (HN, N, C, CA, CB, HA, HB). Overall patch of secondary fold is predicted. One residue (C16) is predicted as β -sheet with low confidence, however this is likely an effect of the disulfide bond affecting the chemical shifts.

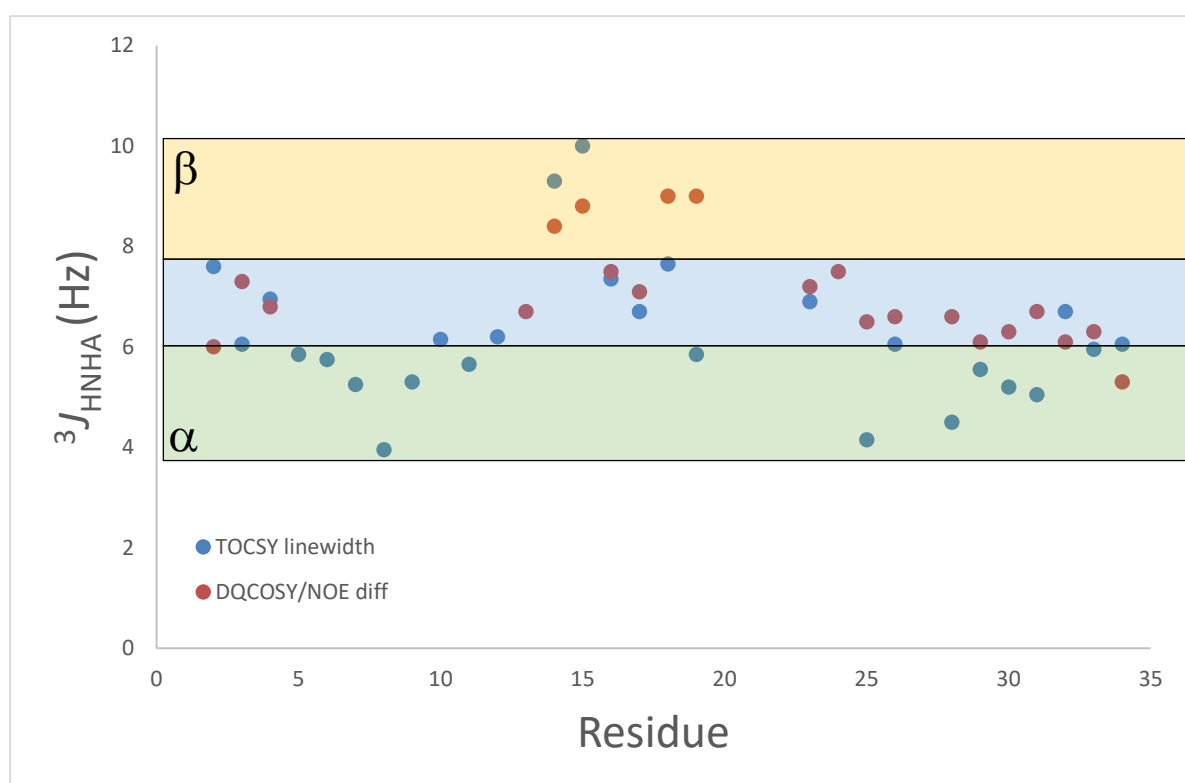


Figure S8. The $^3J_{\text{HNHA}}$ coupling constants for turgencin B_{Mox2} structure estimated using two methods using the TOCSY line widths and the sum/diff displacement of DQF-COSY and NOESY slices. The results indicate access to helical structures (green area) for both sides of the turn, but the couplings also suggest significant conformational averaging (blue area).

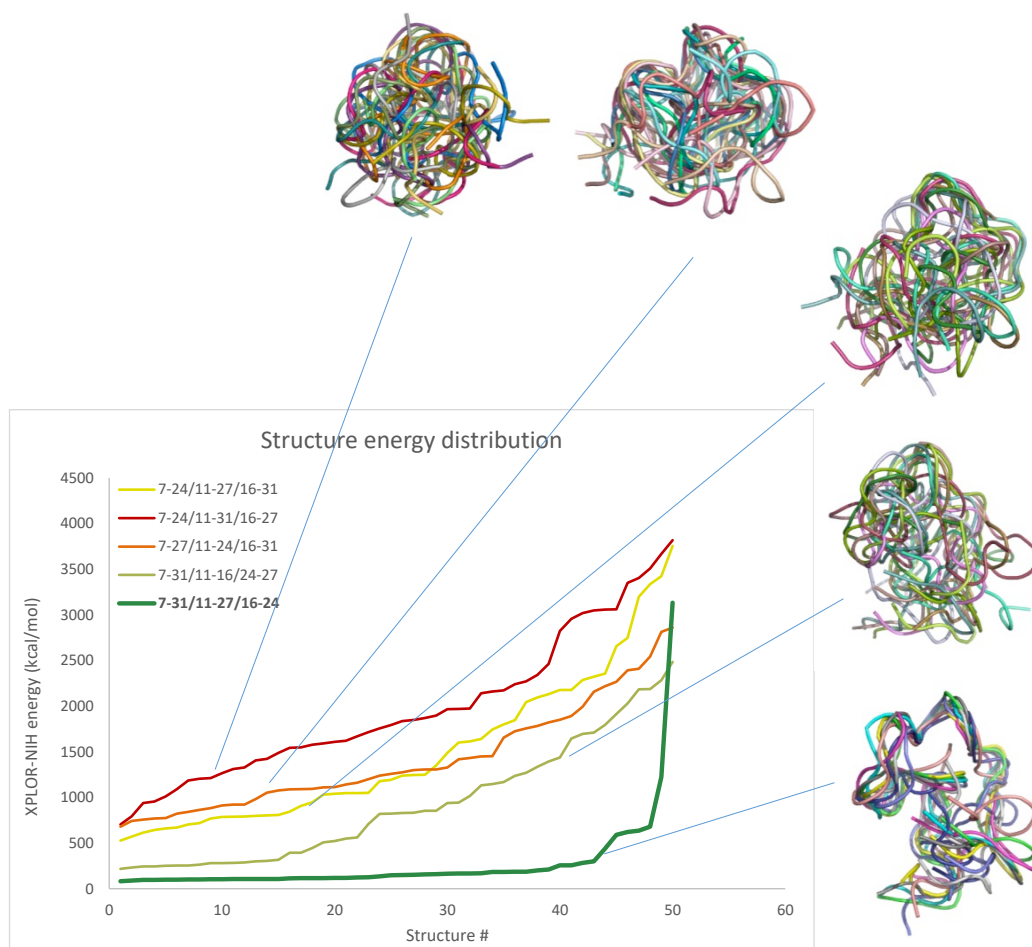


Figure S9. Early test calculations of turgencin B_{Mox2} using crude constraints to evaluate different disulfide patterns using crude constraints. 10 out of 50 structures of each simulation are superimposed, picked at even intervals from the energy profile.

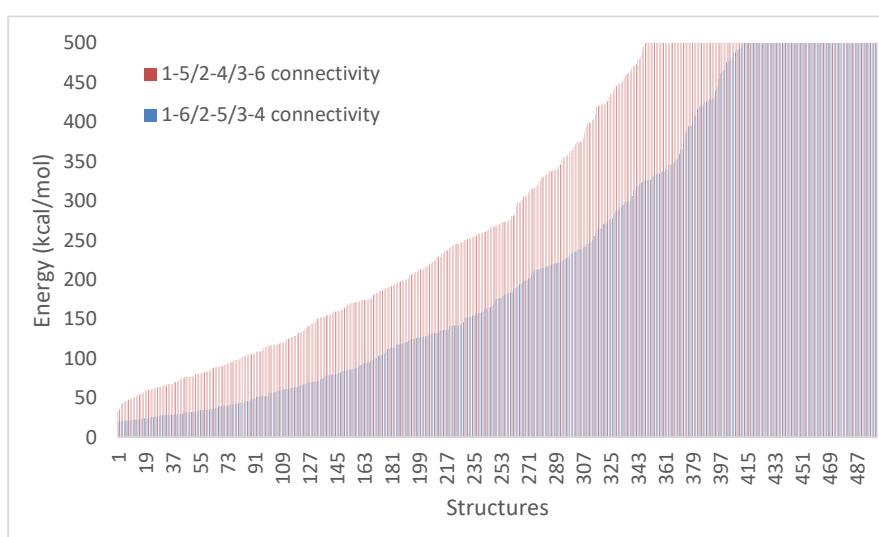


Figure S10. The most viable alternative disulfide pattern of turgencin B_{Mox2} compared to the found pattern in terms of energy of 500 calculated simulated annealing structures using the final constraints.

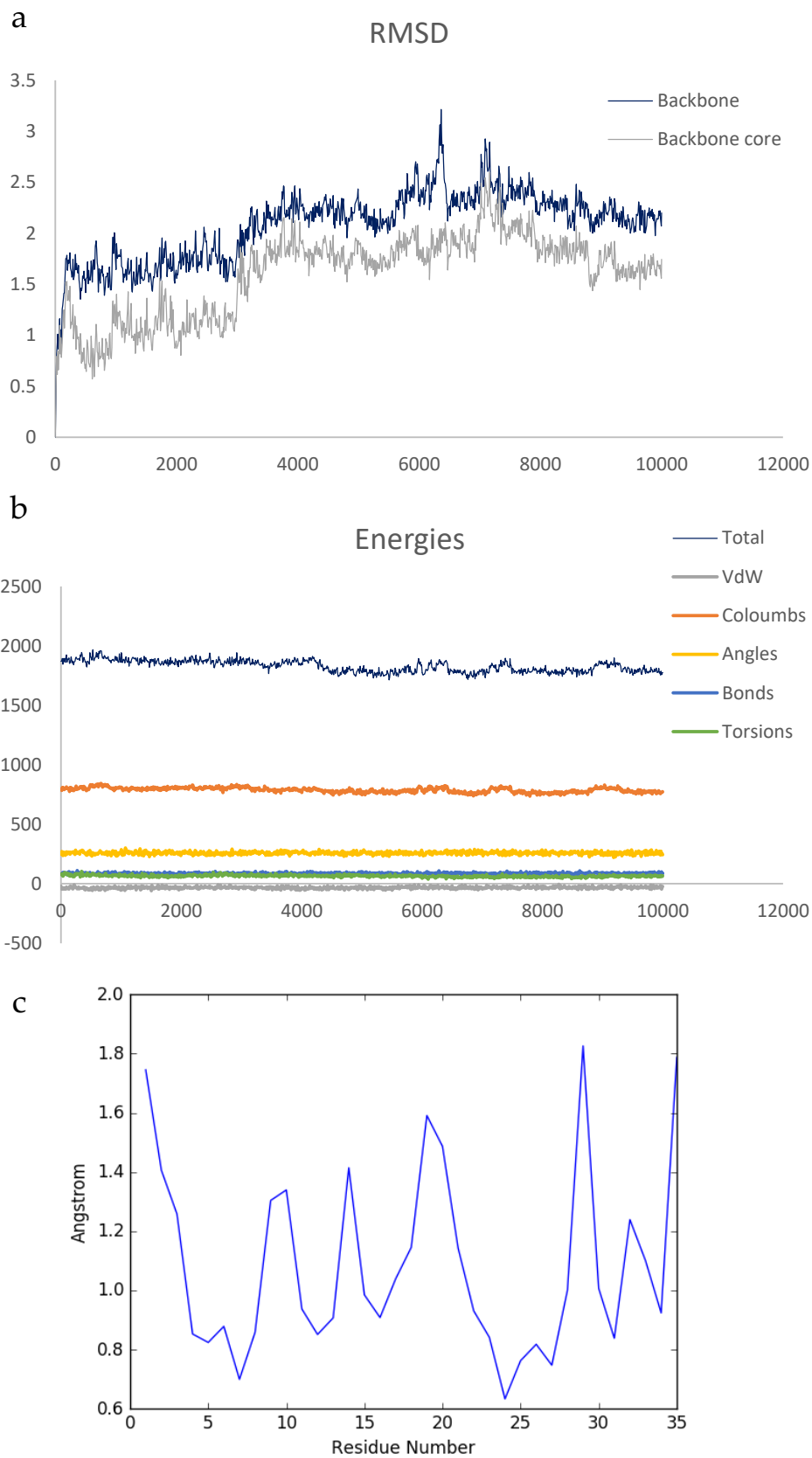


Figure S11. The (a) RMSD relative to the starting frame, (b) energies of turgencin B_{Mox2} and (c) the RMSF of the backbone during the free MD trajectory.

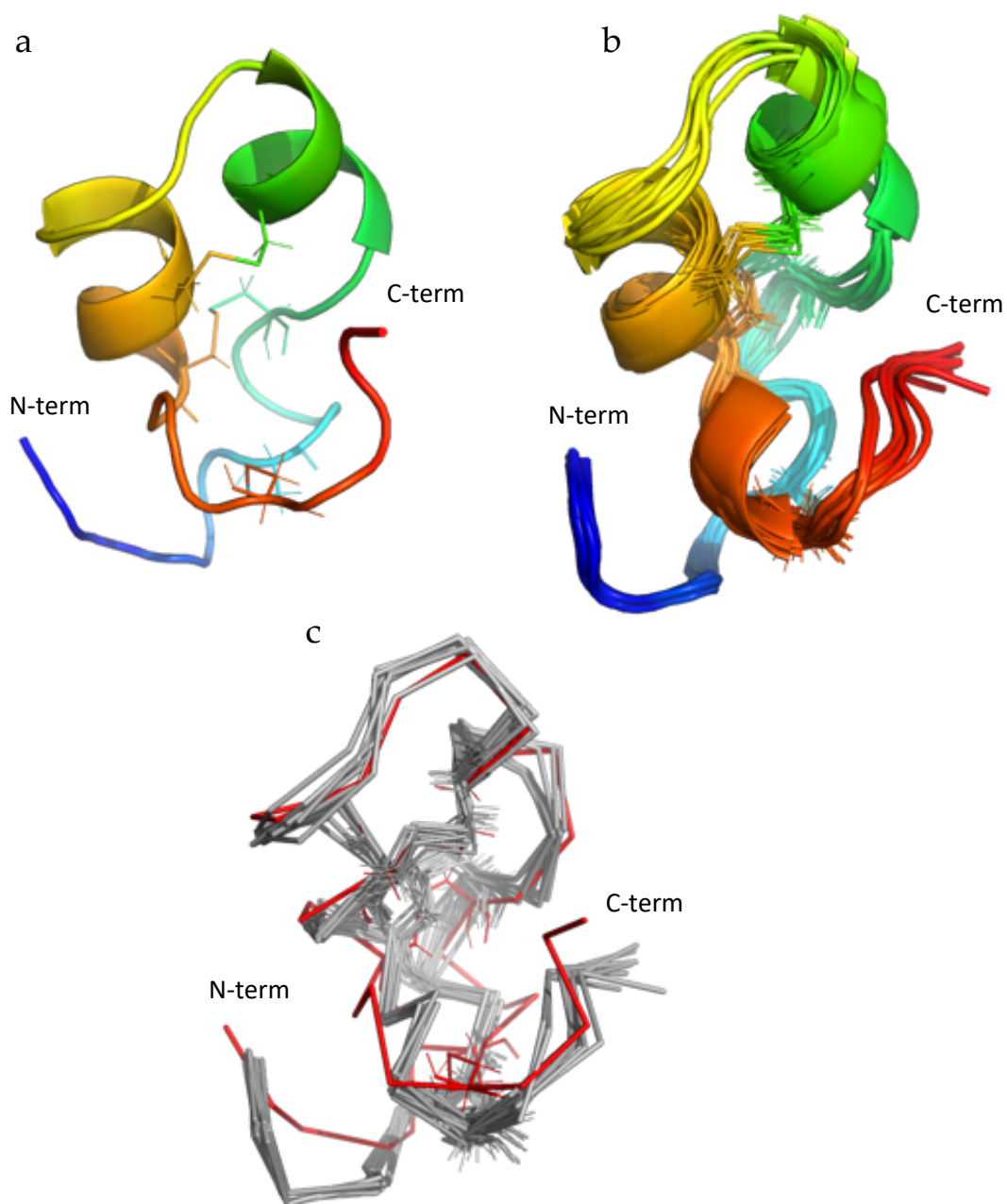


Figure S12. Comparison of NMR and molecular dynamics structures for turgencin B_{Mox2}. (a) The representative NMR structure of turgencin B_{Mox2} selected for MD simulations, and (b) an ensemble sampling the last nanosecond of the simulation. Backbone core (res 6-32) RMSD ~ 1.5 Å. (c) The NMR and MD structures superimposed and displayed with ribbons.

Table S1. Antimicrobial activity of solid phase extract (SPE) fractions and the organic extract. Bacterial test strains: *C. g.* - *Corynebacterium glutamicum*, *B. s.* - *Bacillus subtilis*, *S. a.* - *Staphylococcus aureus*, *E. c.* - *Escherichia coli*, *P. a.* - *Pseudomonas aeruginosa*.

Extract	Antimicrobial activity (MIC; mg/mL)				
	<i>C. g.</i>	<i>B. s.</i>	<i>S. a.</i>	<i>E. c.</i>	<i>P. a.</i>
10% MeCN SPE	1.25	5.00	5.00	10.00	5.00
20% MeCN SPE	2.50	2.50	5.00	5.00	5.00
30% MeCN SPE	0.16	0.16	2.50	5.00	5.00
40% MeCN SPE	0.04	0.08	2.50	5.00	2.50
80% MeCN SPE	0.31	0.31	2.50	5.00	2.50
Organic	2.50	2.50	10.00	>10.00	>10.00

Table S2. Calculated and measured monoisotopic m/z $[M+4H]^{4+}$ ions of turgencin A, turgencin B, and their oxidized derivatives.

Peptide	Calculated monoisotopic mass $[M+4H]^{4+}$	Measured monoisotopic mass $[M+4H]^{4+}$	Error (ppm)
Turgencin A	923.4568	923.4574	0.65
Turgencin A _{Mox1}	927.4555	927.4562	0.71
Turgencin B	885.6526	885.6536	1.11
Turgencin B _{Mox1}	889.6529	889.6532	0.34
Turgencin B _{Mox2}	893.6501	893.6518	1.92

Table S3. Proton chemical shift assignments for turgencin A_{Mox1} in water.

Residue	H (ppm)	H α (ppm)	H β (ppm)	H γ (ppm)	Others (ppm)
GLY ₁	8.56	3.91/3.92			
PRO ₂		4.38	2.24/1.84	2.00/1.94	α :3.50/3.52
LYS ₃	8.61	4.32	1.80/1.70	1.39/1.43	α :1.57/1.58, α :2.90
THR ₄	7.62	4.34	4.41	1.18	
LYS ₅	8.68	3.97	1.82/1.74	1.38/1.40	α :1.66, α :2.94
ALA ₆	8.34	3.99	1.34		
ALA ₇	8.00	4.12	1.39		
CYS ₈	8.16	4.18	3.39/2.96		
LYS ₉	8.58	3.66	1.80/1.69	1.23/1.22	α :1.58/1.56, α :2.90
MET ₁₀	8.16	4.12	2.25	2.94/2.86	α : 1.57, α : 2.62
ALA ₁₁	7.96	4.14	1.49		
CYS ₁₂	8.10	4.45	3.06/3.12		
LYS ₁₃	8.08	3.72	1.99/1.88	1.29	α :1.55, α :2.86
LEU ₁₄	7.63	4.07	1.70/1.55	1.68	α 1:0.78, α 2:0.83
ALA ₁₅	7.77	4.31	1.41		
THR ₁₆	7.77	4.39	4.06	1.04	
CYS ₁₇	8.29	4.21	3.21/2.81		
GLY ₁₈	8.43	3.77/3.74			
LYS ₁₉	7.80	4.26	1.81/1.67	1.36/1.41	α :1.59, α :2.91
LYS ₂₀	7.70	4.75	1.75/1.64	1.26	α :1.63, α :2.90
PRO ₂₁		4.74	1.89/2.38	1.99/1.90	α :3.58/3.34
GLY ₂₂	8.46	3.67/4.01			
GLY ₂₃	7.64	3.76/4.15			
TRP ₂₄	8.42	4.34	3.36/3.18		α 1:7.26, α 1:10.13, α 3:7.43, α 2:7.13, α 2: 7.41, α 3: 7.02
LYS ₂₅	8.02	3.54	1.42/1.26	0.89/0.84	α :1.40, α :2.80
CYS ₂₆	4.17	3.01/2.97			
LYS ₂₇	7.78	3.96	1.74/1.80	1.37/1.29	α :1.54, α :2.84
LEU ₂₈	8.09	3.92	1.46/1.41	1.44	α :0.78/0.74
CYS ₂₉	7.77	4.15	3.34/2.98		
GLU ₃₀	8.43	3.69	2.06/1.88	1.90/2.60	
LEU ₃₁	8.22	4.12	1.72/1.55	1.68	α :0.82/0.81
GLY ₃₂	7.84	3.86/3.85			
CYS ₃₃	7.54	4.66	3.07/2.97		
ASP ₃₄	7.74	4.47	2.68		
ALA ₃₅	7.54	4.27	1.40		
VAL ₃₆	7.53	3.98	2.08	γ 1:0.92, γ 2:0.85	

Table S4. Carbon chemical shift assignments for turgencin A_{MOx1} in water.

Residue	N (ppm)	C α (ppm)	C β (ppm)	C γ (ppm)	Others (ppm)
GLY ₁	109.48	40.56			
PRO ₂		60.50	29.59	24.34	α :46.89
LYS ₃	121.19	53.92	30.14	22.24	α :26.21, α :39.33
THR ₄	111.99	58.48	68.09	19.07	
LYS ₅	123.81	57.34	29.02	22.26	α :26.72, α :39.32
ALA ₆	120.98	52.30	15.32		
ALA ₇	121.95	52.09	15.47		
CYS ₈	121.10	57.05	35.14		
LYS ₉	121.30	57.72	30.13	24.40	α :26.28, α :39.30
MET ₁₀	120.45	52.02	23.24	48.40	α :26.3, α :36.80
ALA ₁₁	123.40	52.42	14.53		
CYS ₁₂	116.13	54.33	35.66		
LYS ₁₃	123.81	56.97	29.22	22.05	α :26.27, α :39.18
LEU ₁₄	118.52	53.97	39.30	24.20	α 1:20.19, α 2:21.16
ALA ₁₅	120.99	50.92	16.46		
THR ₁₆	109.91	61.20	66.78	18.18	
CYS ₁₇	119.35	55.29	40.47		
GLY ₁₈	118.81	43.86			
LYS ₁₉	118.69	54.01	30.64	22.21	α :26.29, α :39.33
LYS ₂₀	117.80	50.79	30.37	22.04	α :26.25, α :39.34
PRO ₂₁		61.75	28.76	24.43	α :47.84
GLY ₂₂	106.81	42.12			
GLY ₂₃	106.85	42.17			
TRP ₂₄	122.69	57.01	25.95	108.03	α 1:124.59, α 2:126.89, α 2:126.20, α 3:117.93, α 2:121.91, α 2:112.01, α 3:119,26, N α 1:129.22
LYS ₂₅	119.54	56.94	28.99	22.57	α :26.31, α :39.15
CYS ₂₆	118.96	55.75	36.82		
LYS ₂₇	120.16	56.37	29.55	22.18	α :26.125, α :39.22
LEU ₂₈	118.33	54.77	39.04	23.94	α :21.82/20.81
CYS ₂₉	119.87	52.41	35.34		
GLU ₃₀	107.90	57.71	26.49	34.96	
LEU ₃₁	121.21	54.92	39.28	24.20	α :22.07

GLY ₃₂	107.37	43.87			
CYS ₃₃	117.92	56.11	33.55		
ASP ₃₄	119.77	53.49	37.87		
ALA ₃₅	121.58	50.23	16.27		
VAL ₃₆	117.53	59.61	29.45	γ 1:17.82, γ 2:18.46	

Table S5. Proton chemical shift assignments for turgencin B_{Mox2} in water.

Residue	H (ppm)	H α (ppm)	H β (ppm)	H γ (ppm)	Others (ppm)
GLY ₁	7.63	3.65, 3.77	-	-	-
ILE ₂	8.65	3.94	1.79	1.19, 1.42, CH ₃ : 0.86	δ CH ₃ : 0.81
LYS ₃	8.43	3.88	1.67, 1.76	1.32, 1.47	δ CH ₂ :1.60, ϵ CH ₂ : 2.89
GLU ₄	8.41	3.82	1.94, 1.98	2.17, 2.25	-
MET ₅	8.01	4.20	2.21, 2.28	2.84, 3.01	ϵ CH ₃ : 2.58
LEU ₆	8.50	3.97	1.420, 1.749	1.74	δ CH ₃ : 0.75, 0.77
CYS ₇	7.83	4.20	2.820, 3.254	-	-
ASN ₈	8.57	4.20	2.701, 2.748	-	-
MET ₉	8.22	4.14	2.24	2.73, 3.02	ϵ CH ₃ : 2.57
ALA ₁₀	7.86	4.21	1.48	-	-
CYS ₁₁	8.01	4.27	3.04, 3.07	-	-
ALA ₁₂	8.22	3.73	1.42	-	-
GLN ₁₃	7.55	4.19	2.06, 2.20	2.40, 2.48	ϵ NH ₂ : 6.85, 7.31
THR ₁₄	7.43	4.50	4.26	1.16	-
VAL ₁₅	8.81	4.09	2.09	0.98, 1.04	-
CYS ₁₆	8.13	4.89	2.76, 3.31	-	-
LYS ₁₇	7.23	3.99	1.70	1.30	δ CH ₂ :1.60, ϵ CH ₂ : 2.90
LYS ₁₈	8.13	4.17	1.70, 1.80	1.31	δ CH ₂ :1.60, ϵ CH ₂ : 2.89
SER ₁₉	7.77	4.37	3.76, 3.83	-	-
GLY ₂₀	8.18	3.82, 4.12	-	-	-
GLY ₂₁	8.62	3.85, 4.44	-	-	-

PRO ²²	-	4.26	1.87, 2.30	1.90, 1.98	δCH_2 : 3.54, 3.68
LEU ²³	8.46	4.09	1.34, 1.70	1.60	δCH_3 : 0.80, 0.84
CYS ²⁴	7.50	4.19	3.16, 3.21	-	-
ASP ²⁵	8.39	4.25	2.62, 2.67	-	-
THR ²⁶	8.34	3.86	4.08	1.17	-
CYS ²⁷	7.56	4.16	3.01, 3.36	-	-
GLN ²⁸	8.29	3.93	1.99, 2.02	2.22, 2.61	-
ALA ²⁹	8.38	4.02	1.41	-	-
ALA ³⁰	7.64	4.15	1.46	-	-
CYS ³¹	7.49	4.55	3.00, 3.08	-	-
LYS ³²	7.63	4.03	1.79, 1.85	1.36, 1.49	δCH_2 : 1.59, ϵCH_2 : 2.86
ALA ³³	7.57	4.21	1.37	-	-
LEU ³⁴	7.61	4.15	1.45, 1.75	1.78	δCH_3 : 0.78, 0.82
GLY ³⁵	7.93	3.78, 3.87	-	-	terminal-NH ₂ : 7.05, 7.21

Table S6. Carbon chemical shift assignments for turgencin B_{Mox2} in water.

Residue	N (ppm)	C α (ppm)	C β (ppm)	C γ (ppm)	Others (ppm)
GLY ₁	-	61.014	-	-	-
ILE ₂	122.15	60.82	35.45	14.68, 25.64	δCH_3 : 10.32
LYS ₃	120.82	57.24	29.27	22.65	δCH_2 : 26.37 ϵCH_2 : 39.28
GLU ₄	120.90	57.43	26.15	33.18	-
MET ₅	118.83	55.76	23.13	48.73	ϵCH_3 : 36.56
LEU ₆	121.07	55.31	38.68	23.92	δCH_3 : 19.85, 22.68
CYS ₇	121.22	57.19	32.11	-	-
ASN ₈	120.64	54.04	35.91	-	-
MET ₉	120.49	55.60	22.93	47.84	ϵCH_3 : 36.547
ALA ₁₀	122.84	52.64	14.45	-	-
CYS ₁₁	116.93	54.80	35.20	-	-
ALA ₁₂	123.91	52.69	15.50	-	-
GLN ₁₃	111.92	53.47	27.05	31.25	δCO : 177.40
THR ₁₄	108.63	57.095	67.66	18.38	-
VAL ₁₅	118.30	61.24	29.56	17.42, 19.53	-
CYS ₁₆	116.07	52.91	41.12	-	-

LYS ₁₇	120.89	56.09	30.06	22.133	δCH ₂ : 26.35 εCH ₂ : 39.32
LYS ₁₈	117.66	54.22	29.95	22.18	δCH ₂ : 26.34 εCH ₂ : 39.29
SER ₁₉	113.19	55.42	61.55	-	-
GLY ₂₀	108.86	42.22		-	-
GLY ₂₁	110.51	42.04		-	-
PRO ₂₂	-	62.77	29.46	24.59	δCH ₂ : 47.00
LEU ₂₃	117.91	55.08	38.44	24.45	δCH ₃ : 20.31, 22.08
CYS ₂₄	119.23	55.88	36.38	-	-
ASP ₂₅	120.78	54.79	36.90	-	-
THR ₂₆	116.55	63.82	66.02	18.78	-
CYS ₂₇	123.34	58.41	35.90	-	-
GLN ₂₈	116.81	56.55	25.79	32.02	-
ALA ₂₉	123.12	52.24	15.11	-	-
ALA ₃₀	121.61	51.88	14.65	-	-
CYS ₃₁	115.49	52.02	32.63	-	-
LYS ₃₂	119.51	55.41	29.82	22.31	δCH ₂ : 26.24, εCH ₂ : 39.20
ALA ₃₃	121.34	50.37	15.71	-	-
LEU ₃₄	118.72	53.19	39.37	23.84	δCH ₃ : 20.26, 23.08
GLY ₃₅	108.32	42.36	-	-	-

Table S7. Peptides sharing the same disulfide connectivity as turgencin B (C1-C6/C2-C5/C3-C4).

AMP	#aa	Sequence and protein data bank (PDB) ID	Species	Ref.
Turgencin B	35	GIKEMLCNMACAQTVCCKKSGGPLCDTCQAACKAL-NH ₂	<i>Synoicum turgens</i> (ascidian)	This work
TEWP	36	pEKKCPGRCTLKCGKHERPTLPYNCGKYICCVPVKVK (PDB: 2B5B)	<i>Caretta caretta</i> (Loggerhead sea turtle)	[1]
Pelovaterin	42	DDTPSSRCGSGGWGPCLPVDLLCIVHVTVGCSGGFGCCRIG (PDB: 2JR3)	<i>Pelodiscus sinensis</i> (Chinese softshell turtle)	[2]
Caenopore-5	81	RSALSCQMCELVVKKYEGSADKDANVIKDFDAECKKLFHTIPFGTRECDHYVNSKVDPIIHELEGGTAPKDVCTKLNECP (PDB: 2JS9)	<i>Caenorhabditis elegans</i> (nematode)	[3]
NK-lysin	78	GLICESCRKIIQKLEDMVGPQPNEDTVTQAASRVCDKMKILRGVCKKIMRTFLRRISKDILTGKKPQAIKVDIKICE (PDB: 1NKL)	<i>Sus scrofa</i> (pig)	[4]
RTD-1	18	GF CRCLCRRGVCR CIC TR (cyclic, 3 DSB + head to tail peptide bonds) (PDB: 2LYF)	<i>Macaca mulatta</i> (Rhesus monkey)	[5], [6]
Viscotoxin A3	46	KSCCPNTTGRNIYNACRLTGAPRPTCAKLSCCKIISGSTCPSDY PK (PDB: 1ED0)	<i>Viscum album</i> (mistletoe)	[7] (sequence), [8] (activity)

References

1. Chattopadhyay, S.; Sinha, N. K.; Banerjee, S.; Roy, D.; Chattopadhyay, D.; Roy, S., Small cationic protein from a marine turtle has β -defensin-like fold and antibacterial and antiviral activity. *Proteins* **2006**, 64, 524-531.
2. Lakshminarayanan, R.; Vivekanandan, S.; Samy, R. P.; Banerjee, Y.; Chi-Jin, E. O.; Teo, K. W.; Jois, S. D. S.; Kini, R. M.; Valiyaveetil, S., Structure, self-assembly, and dual role of a β -defensin-like peptide from the Chinese soft-shelled turtle eggshell matrix. *J. Am. Chem. Soc.* **2008**, 130, 4660-4668.
3. Mysliwy, J.; Dingley, A. J.; Stanisak, M.; Jung, S.; Lorenzen, I.; Roeder, T.; Leippe, M.; Grötzinger, J., Caenopore-5: The three-dimensional structure of an antimicrobial protein from *Caenorhabditis elegans*. *Developmental & Comparative Immunology* **2010**, 34, 323-330.
4. Liepinsh, E.; Andersson, M.; Ruysschaert, J.-M.; Otting, G., Saposin fold revealed by the NMR structure of NK-lysin. *Nature Structural Biology* **1997**, 4, 793-795.
5. Tang, Y.-Q.; Yuan, J.; Ösapay, G.; Ösapay, K.; Tran, D.; Miller, C. J.; Ouellette, A. J.; Selsted, M. E., A cyclic antimicrobial peptide produced in primate leukocytes by the ligation of two truncated α -defensins. *Science* **1999**, 286, 498-502.
6. Selsted, M. E., θ -defensins: Cyclic antimicrobial peptides produced by binary ligation of truncated α -defensins. *Current Protein & Peptide Science* **2004**, 5, 365-371.
7. Romagnoli, S.; Ugolini, R.; Fogolari, F.; Schaller, G.; Urech, K.; Giannattasio, M.; Ragona, L.; Molinari, H., NMR structural determination of viscotoxin A3 from *Viscum album* L. *Biochem. J.* **2000**, 350, 569-577.
8. Giudici, A. M.; Regente, M. C.; Villalaín, J.; Pfüller, K.; Pfüller, U.; De La Canal, L., Mistletoe viscotoxins induce membrane permeabilization and spore death in phytopathogenic fungi. *Physiologia Plantarum* **2004**, 121, 2-7.